



European volcanological supersite in Iceland: a monitoring system and network for the future

Report

D6.3 - Tremor characteristics and array processing

Work Package:	<i>Imminent eruptive activity, eruption onset and early warning</i>		
Work Package number:	6		
Deliverable:	<i>Tremor characteristics and array processing</i>		
Deliverable number:	6.3		
Type of Activity:	RTD		
Responsible activity leader:	K. S. Vogfjörð		
Responsible participant:	IMO		
Authors:	Eva Eibl (UCD), Christopher Bean (UCD), K. S. Vogfjörð (IMO)		

Type of Deliverable:	<i>Report</i>	<input checked="" type="checkbox"/>	<i>Demonstrator</i>	<input type="checkbox"/>
	<i>Prototype</i>	<input type="checkbox"/>	<i>Other</i>	<input type="checkbox"/>
Dissemination level:	<i>Public</i>	<input checked="" type="checkbox"/>	<i>Restricted Designated Group</i>	<input type="checkbox"/>
	<i>Prog. Participants (FP7)</i>	<input type="checkbox"/>	<i>Confidential (consortium)</i>	<input type="checkbox"/>

Seventh Framework Programme
EC project number: 308377



Summary

The objective of this deliverable was to help minimise the number of false alarms associated with eruption and flood forecasts at glacier covered volcanoes. As seismic tremor signals often precede such hazardous events, the approach was to determine and draw a distinction between the characteristics of the various processes capable of generating continuous seismic tremor signals. In particular the aims were to compare and contrast subglacial eruptions, floods and boiling hydrothermal systems in terms of the tremor signals generated.

Tremor signals are usually emergent and cannot be located using traditional methods associated with P and S-wave picks. In contrast 'tight clusters' of seismic stations (called seismic arrays) can be used to estimate the apparent propagation speed (or more precisely its inverse, apparent slowness), and propagation direction of tremor signals, allowing them to be located in 3D space. FutureVolc's Milestone 48 saw the installation of two continuously streaming seismic arrays west of Vatnajökull (Vatna Glacier). Here D6.3 demonstrates some of the signals recorded on these arrays, and explains the processing and interpretation of the signals they record in terms of our understanding of seismic tremor generation and our ability to interpret tremor in terms of specific geophysical processes.

Introduction

Seismic tremor signals are viewed with considerable interest as a precursor to eruptions and/or flooding events (jökulhlaup) on glacier covered volcanoes. Changes of tremor occurrence rate, amplitude and frequency have been hypothesized as early indicators of imminent volcanic eruptions, of subglacial flooding and of ice-water interaction during hydrothermal boiling episodes. Tremor signals are usually emergent and cannot be located using traditional methods associated with P and S-wave picks. In contrast 'tight clusters' of seismic stations (called seismic arrays) can be used to estimate the apparent slowness and propagation direction of tremor signals, allowing them to be located in 3D space. At the commencement of the FutureVolc project two continuously streaming (data streamed back to Icelandic Met Office (IMO)) seismic arrays – with 7 seismic stations each – were installed west of Vatnajökull, with the aim of capturing an expected flooding event from the western Cauldrons. The two array locations at Jökulheimar and Innri-Eyrar respectively are given in Figure 6.3.1. The idea was to identify the specific tremor characteristics associated with a known geophysical processes (flooding in this case), to be used as a reference for identifying future flooding events from fewer stations from the national seismic network both at Vatnajökull and at other locations. That event eventually came late in the project (October 2015) and was recorded on the seismic arrays. Furthermore, due to increased seismic activity beneath Vatnajökull, a third array was installed just north of the glacier, at Urðarháls 14km west of the eruptive fissure, immediately prior to the Holuhraun eruption. This had given us a unique opportunity to study tremor associated magma movement and with the eruption itself.

Rationale for array installation

As arrays are the best means of locating seismic tremor, at the concept stage in the development of the FutureVolc proposal the new arrays were envisaged with the aim of tracking the speed of the migration of the tremor signal, to determine if it is related to flooding or lava flow. Evidence suggests that during a flood, the flood front is retarded and water 'piles up' behind this front (Roberts, 2005) which we suggest then likely acts as the dominant source of seismic tremor. The flood front commonly moves at a speed of 1-2m/s (Einarsson, 2009; Vogfjörð et al., 2006). The extrusion of lava under ice will cause a 'water boiling signal' so there is also a hypothesized 'boiling signal' associated with the process which generates tremor. However this is likely a quasi-stationary

source, but lava moves at speeds on the order of mm/s: e.g. Eyjafjallajökull 2011, ~3mm/s (Oddsson et al., 2011). Hence there is a three orders of magnitude difference in the speed of a migrating flood front versus migrating lava. Therefore tracking the speed of tremor migration should allow us to discriminate between flood water ('fast'), lava on the move ('slow') and hydrothermal boiling ('stationary'). At the concept phase specifically designed and bespoke built glacier seismometers capable of handling high levels of tilt were also envisaged as part of the available instrumentation. However that component was delayed due to technical problems with the equipment, and is not included herein.

Tremor location method using array techniques

As tremor has no clear P and S wave arrivals traditional travel time location methods cannot be applied in order to locate the source. Amplitude location methods is one possible approach but due to a sparse station network and inter-station distances of a few tens of kilometers the location would have a big uncertainty. A network of closely spaced seismometers (a 'seismic array') can be used to determine the source location more reliably as the processing of the data allows the determination of the direction of the arriving waves.

For a joint determination of back azimuth and slowness of a wave frequency domain (Capon, 1969; Schmidt, 1986; Goldstein and Archuleta, 1987) and time domain methods exist (Frankel et al., 1991; Del Pezzo et al., 1997; Saccorotti and Del Pezzo, 2000). Methods were contrasted in the literature (e.g. in Almendros et al. (2014), Rost and Thomas (2002) and we chose to perform a frequency wavenumber (FK) analysis with a moving time window (see early reference, Capon, 1969). The FK analysis is a beamforming method in the spectral domain that performs a grid search with a horizontal slowness (inverse of velocity) grid and various back azimuths. Advantages of FK analysis is that it is performed in the spectral domain and is faster than time domain methods. Additionally it is more objective as covariance matrices are calculated.

Based on the array response of our arrays we chose a slowness grid in x and y with a limit of ± 0.6 s/km and a stepsize which is one quarter the width of the main lobe at half height. The stepsize depends on the amount of stations and is, for 7 stations, a minimum of 0.02 s/km. The whole dataset is cut into a few minutes to one hour long time windows. We detrend, taper, instrument correct, filter and downsample the vertical component of the data to a sampling frequency of 20 Hz. During the array processing the time window is subdivided into smaller, overlapping time windows of at least three periods length in which the standard FK analysis is performed. The result is a time series of back azimuth, slowness, relative and absolute power of the predominant signal in each time window. Changes in the resulting back azimuths or slownesses can then reveal different phases in a signal or different events. In order to create maps indicating the source location we created histograms of backazimuth and slowness and picked the maximum. For local events we used the first point in time where the relative power exceeded 0.93.

Testing the array methodology using local earthquakes

Whilst array methods are very suitable for locating seismic tremor, they can also be used to locate 'standard' earthquakes. This gives us the opportunity to test the performance of our arrays and the analysis methodology. We do this by comparing the array derived locations of earthquakes with the locations of the same events determined by the SIL seismic network operated by IMO.

The Holuhraun eruption (August 2014 to February 2015) was preceded and accompanied by 72 earthquakes which had magnitudes above 5. Those events all occurred on the ring fault of the Bárðarbunga caldera at 1-7 km depth according to relative locations but depth determination has an uncertainty of a few kilometers. Locations are not as precise as for magnitude 2 to 3 events due to very emergent onsets, long source time functions so that S-wave arrivals are difficult to determine and many events are clipped at the closest stations. Yet from an array processing perspective, the signal-to-noise ratio is high for these $M=5+$ events. Figure 6.3.1 shows the location of a $M=5.2$ event that was recorded by only 2 arrays to the west – it occurred before the installation of the 3rd northern array. The point of the highest probability (green dot, at the intersection of the two most probably back azimuths of the P-waves, marked by red lines) is in excellent agreement with the IMO location based on the national SIL network ($< 1\text{km}$ difference in x-y). Given that the SIL location also has an associated error we take this as confirmation that the arrays are performing well. However it can be seen that the location has an error ellipse elongated in northeast-southwest direction, which is a function of the array locations relative to the seismic event. Observed slownesses were 0.08 s/km at Jökulheimar and 0.04 s/km at Innri-Eyrar. Such values indicate steeply dipping body waves, consistent with a deep source, as further discussed below.

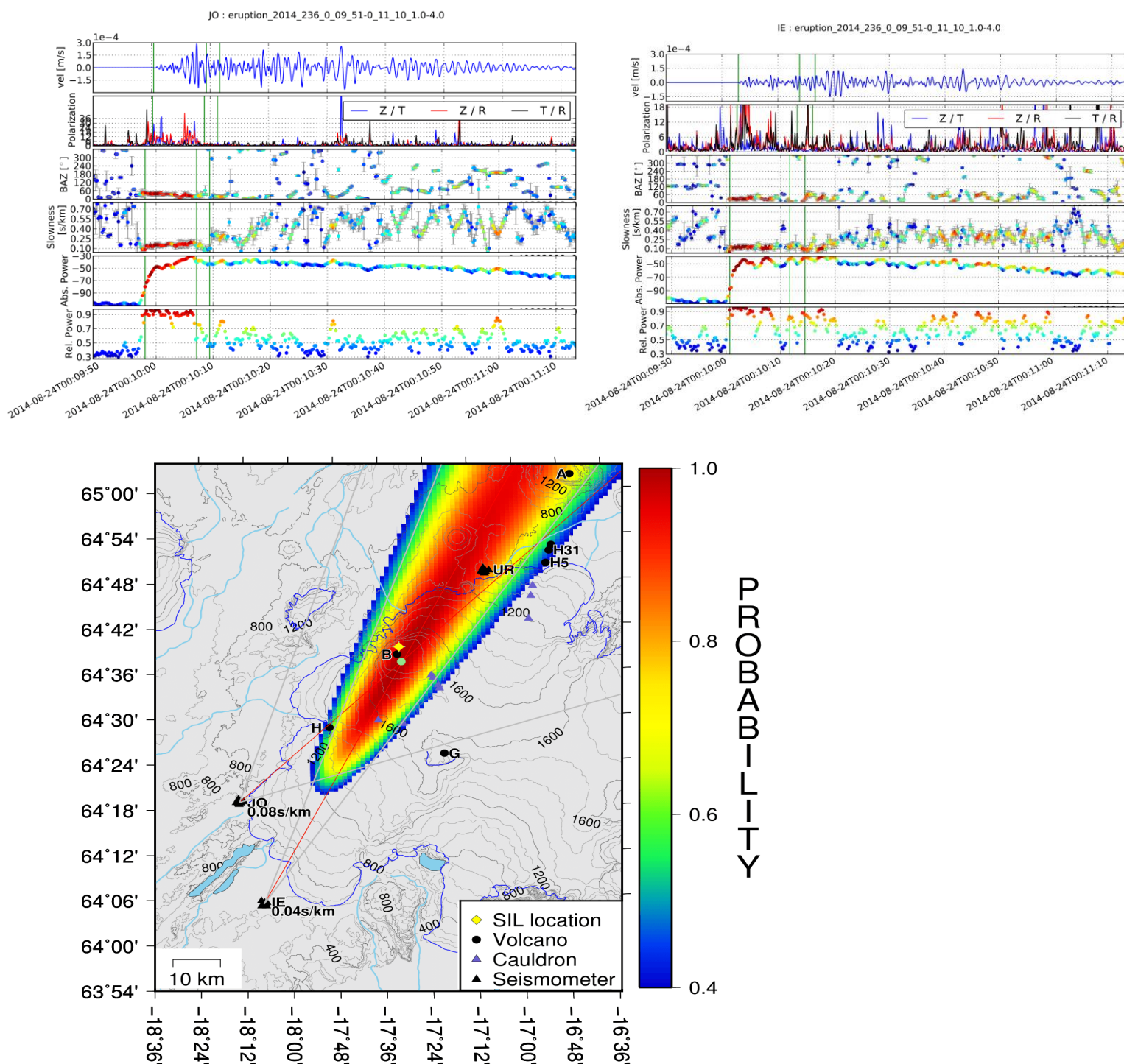
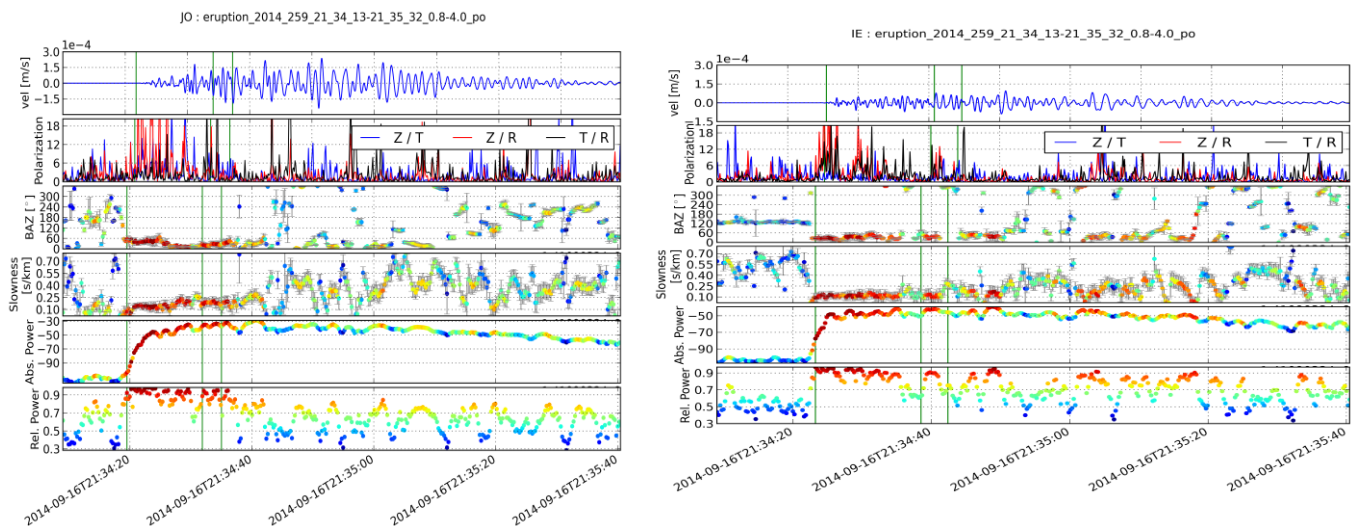


Figure 6.3.1: Magnitude 5.3 earthquake on August 24th, 2014 at 5.3 km depth at the Bárðarbunga caldera located with the IMO network and JO and IE arrays. All points with a semblance of less than 0.3 were discarded. (top left (a), top right (b)) Instrument corrected, 1 to 4 Hz filtered, vertical seismogram of the event on station JOK, polarisation of the wavefield and results from the FK analysis in time (BAZ, slowness, absolute and relative power). Vertical green lines indicate the arrival of the P wave (p) and expected arrival times for S (s) and surface waves (su) based on a $v_p/v_s = 1.78$ and $v_{su}/v_s = 0.9$ for (a) Jökulheimar and (b) Innri-Eyrar. (bottom panel (c)) Result from array analysis plotted on top of topography. The time of the first point with relative power above 0.9 was used to pick the back azimuth and slowness of the event. The green point marks the point with the highest probability; the yellow diamond the location from the SIL catalogue. Red lines indicate the BAZ at each array, the grey line give the error depending e.g. on the amount of available stations. Marked volcanoes are Bardarbunga (B), Askja (A), Grimsvotn (G), Hamarinn (H). Holuhraun eruption sites 15 km south of Askja are marked with H as well; cauldrons with purple triangles.

Most of the earthquakes and tremor were only recorded by two arrays. For some events though we have recordings from three arrays which reduces the error ellipse significantly as we show in figure 6.3.2. The location is based on the back azimuth of the arrival of the P wave. The third array helps to constrain the event location but an elongation in northeastern-southwestern direction is still visible, as unfortunately two of the arrays and the event are almost co-linear. Slownesses were 0.06 s/km in Jökulheimar, 0.09 s/km in Innri-Eyrar and 0.16 s/km in Urðarháls and indicate body waves which have a steeper incidence angles at both Jökulheimar and Innri-Eyrar.



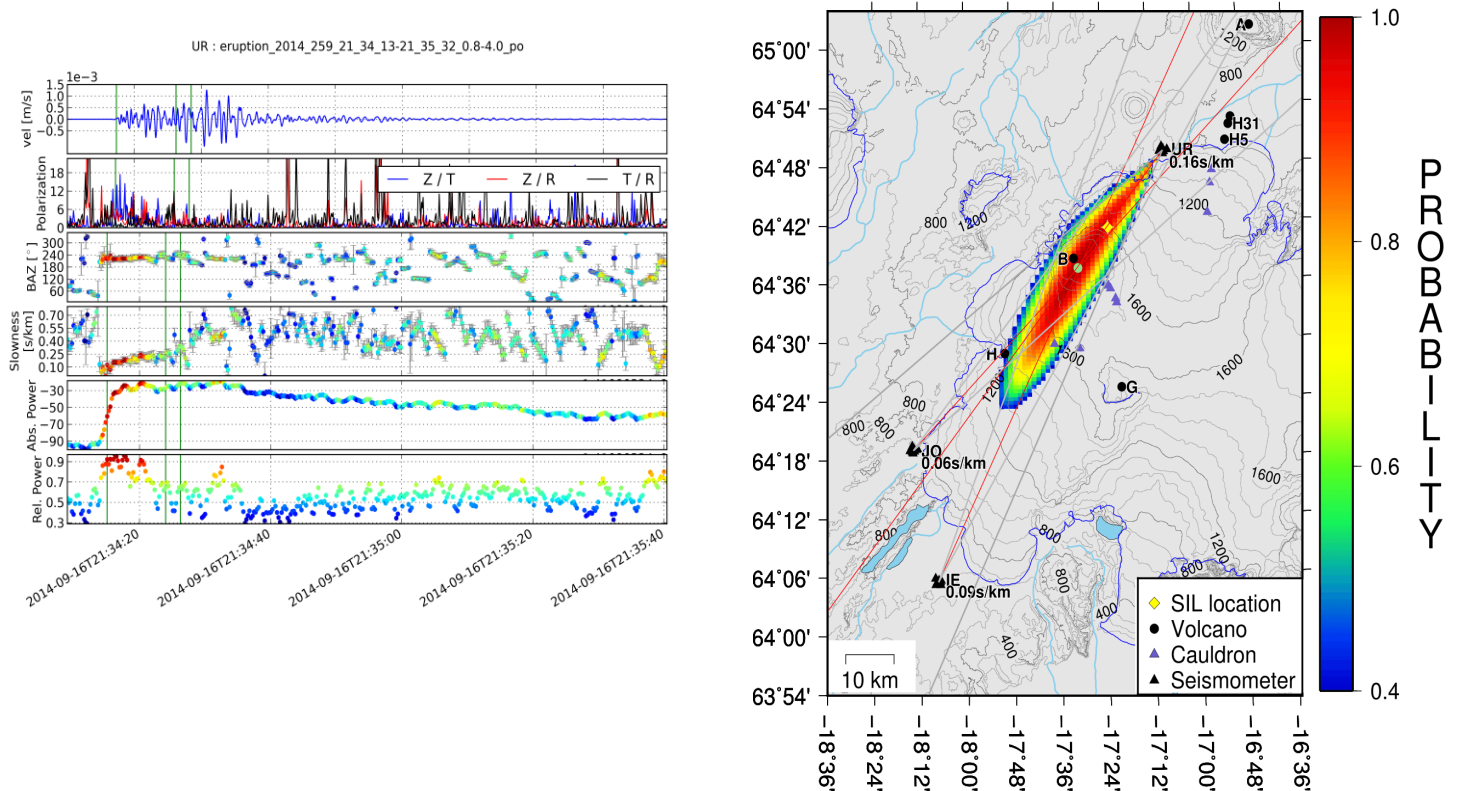


Figure 6.3.2: Magnitude 5.4 earthquake on September 16th, 2014 in 7 km depth at the Bárðarbunga caldera located with the IMO network and JO, IE and UR arrays. All points with a semblance of less than 0.3 were discarded. (a-c) Instrument corrected, 0.8 to 4 Hz filtered, vertical seismogram of the event on station JOK, polarisation of the wavefield and results from the FK analysis in time (BAZ, slowness, absolute and relative power). Vertical green lines indicate the arrival of the P wave and expected arrival times for S and surface waves based on a $v_p/v_s = 1.78$ and $v_{su}/v_s = 0.9$ for (top left (a)) Jökulheimar, (top right (b)) Innri-Eyjar and (bottom left (c)) Urðarháls. (bottom right (d)) Result from array analysis plotted on top of topography. Marks as in figure 1.

Again, as in figure 6.3.1, there is a good correlation between the array derived and seismic network derived locations.

Seismic wavefield analysis of M5 events, using seismic arrays.

The M=5+ events also offer an opportunity for us to test our ability to characterize other wavefield properties, using arrays. All 72 events with a magnitude of at least 5 were used to study the slownesses associated with different wave types (P, S and Surface waves). The rationale for this analysis is so that we can use this information to better understand the depth and wavefield content of seismic tremor as determined by array analysis. Currently this type of detailed information about the seismic tremor is unknown. Slownesses were manually picked from the slowness diagrams for each event.

According to:

$$\text{slowness} = 1 / V_{\text{app}} = \sin(i)/V_c \quad (6.3.1)$$

it is possible to link observed (apparent) slownesses ($1/V_{app}$) to the velocity of the medium underneath the array (V_c) and to i , the incidence angle of the incoming wave beneath the array.

From this analysis we can derive typical slownesses associated with different wavetypes. For surface waves we observed slownesses around 0.7 s/km, for body waves they depend on the incidence angle and were between 0.08 and 0.1 s/km for steeply arriving P waves. This information can be used when studying a tremor pulse. The slownesses can indicate the wave type which can then be used to deduce the depth of the source.

Locations of seismic events (earthquakes) beneath the Skafta Cauldrons

As we expected a flood from the eastern cauldron we also tested the ability of the arrays to locate events in the eastern and western cauldrons. Figures 6.3.3(a) and (b) show an earthquake in December 2013 underneath the western cauldron that was recorded by both western arrays. The event clearly arrives earlier at the Jökulheimar array which is consistent with the back azimuth given by the array analysis. Figures 6.3.3(c) and (d) show the relative power, absolute power, back azimuth and slowness in time which is the output from the FK analysis. The arrival of the event is clearly visible as an increase in relative and absolute power and a more stable back azimuth and slowness. In order to create figure 6.3.3(e) the back azimuth and slowness at the time of the first relative power above 0.93 were picked. The yellow diamond indicates the location from the IMO network which is near the two back azimuths from our arrays. These tests revealed that the array location technique works well for events with magnitudes of 1 or 2, in the Skafta region.

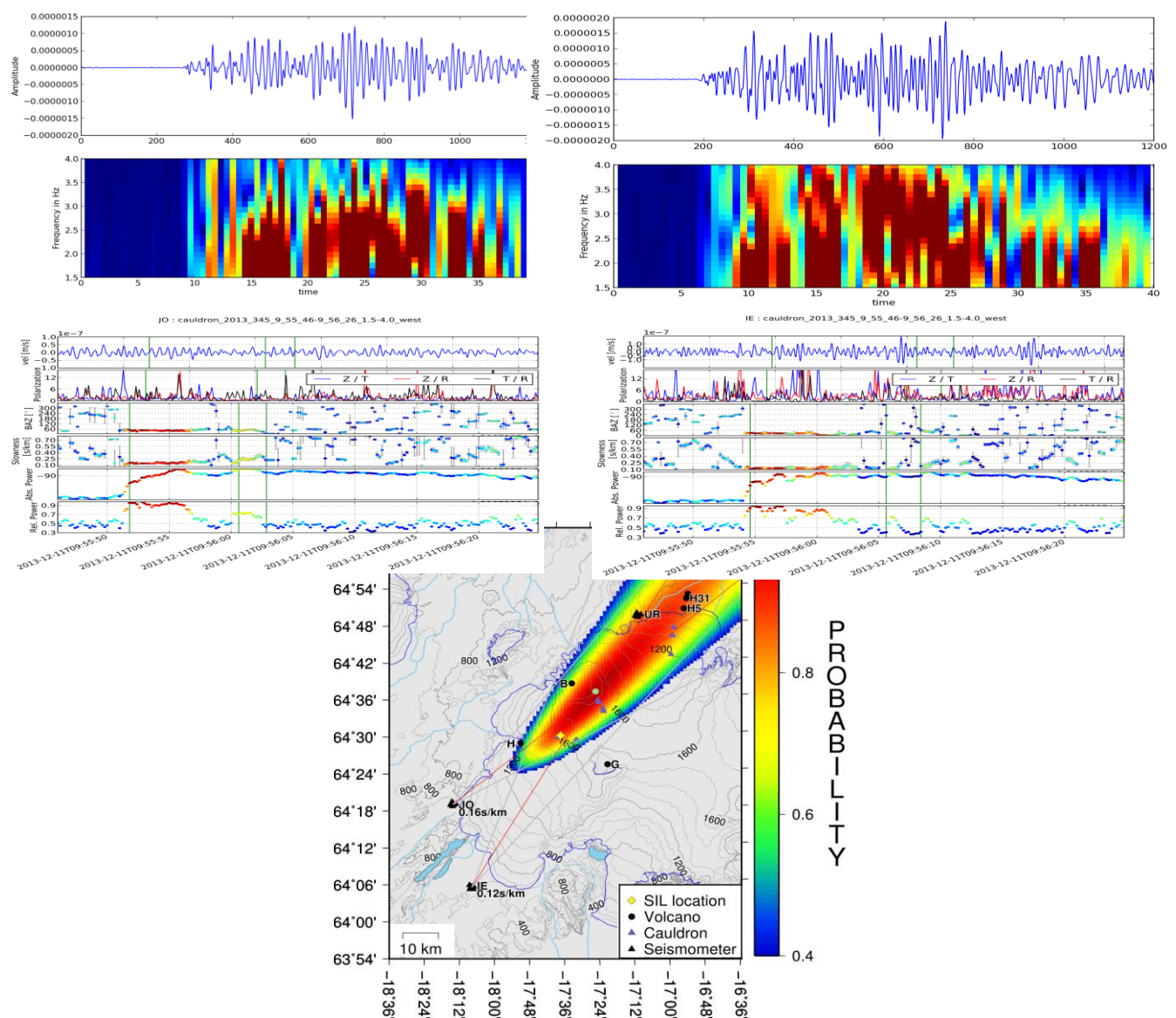


Figure 6.3.3: M 1.9 shallow earthquake in the western Skafta cauldron on December 11th, 2013. IMO location using a standard network is marked with a yellow diamond in the bottom panel (e). All points with a semblance of less than 0.3 were discarded. Instrument corrected seismogram and spectrogram of the event on (top left (a)) station JOK from the Jökulheimar array (JO) and (top right (b)) station IEY from the Innri-Eyrar array (IE). Bottom left (c) & bottom right (d) show results from the FK analysis in time for Jökulheimar & Innri-Eyrar, respectively. The event is clearly visible in an increased relative and absolute power and a very stable back azimuth and slowness. (e) Result from array analysis plotted on top of topography. The time of the first arrival of the P wave was used to pick the back azimuth and slowness of the event.

Continuous Array Processing from August 2014 to February 2015

In the previous section we looked at selected events in order to determine wavefield characteristics, near-array velocities and array location performance. Now, in order to get an overview of the dataset from the arrays we divided the dataset from August, 16th 2014 until February 27th 2015 into one hour long, non-overlapping time windows. For each hour we determined back azimuth, slowness, relative and absolute power in 20% overlapping time windows whose duration were 30 times, the inverse of the central frequency. We chose to average 30 periods of tremor in order to increase the coherency of the signal. The lower limit for the relative power was set to 0.25 in a frequency band of 0.8-2.4 Hz. For all slownesses and back azimuths we then created histograms with 0.002 s/km and 0.5° wide bins, respectively and picked the maximum as predominant back azimuth. We decided to use this approach as the values do not stabilise as much as for earthquakes. Results for the period August, 16th to September 26th 2014 are shown in figure 6.3.4.

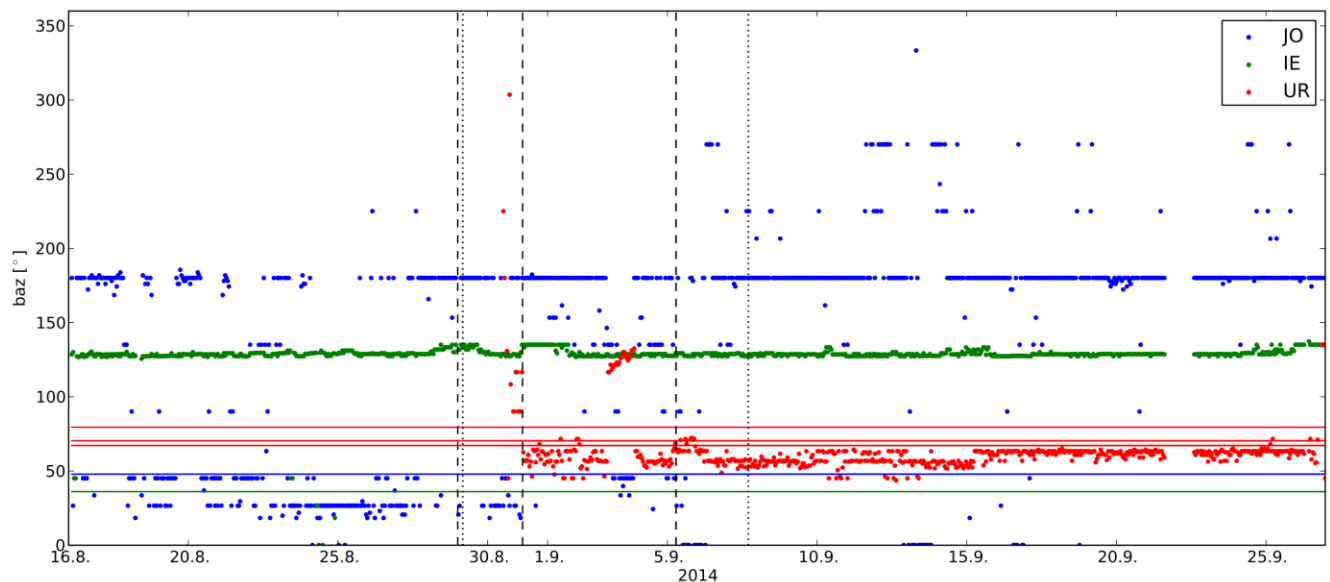


Figure 6.3.4: Overview of the predominant back azimuth in 1 hour long time windows in August and September 2014 obtained from FK analysis performed in the 0.8-2.4 Hz band. We mark the beginning of an eruption with a black dashed line. The end of an eruption with a black dotted line. The green and blue horizontal lines indicate the expected back azimuths for a signal from the Holuhraun fissures at Innri Eyra and Jökulheimar array, respectively. Urðarhál is shown in red. As Urðarhál is closest to the eruptive site the array could distinguish tremor coming from the eruptive fissure on August 31st and the fissure active on September 5th-7th. The three red lines mark, with decreasing back azimuth, the fissure on September 5th, the southernmost and northernmost end of the eruptive fissure.

We installed the third array in Urðarhál on August 30th, 2014 at only 14 km distance from the eruptive site. JO is 90 km from the Holuhraun fissure, IE 105 km. We see a stabilisation of the back azimuth with the beginning of the eruption on August 31st. On the first two days of the eruption back azimuths at UR are between 45° to 63°. Until September 15th it seems to stabilise around 56° and changes to around 62°. Remarkable is September 3rd when the back azimuth jumps to 115° and gradually changes during the day to 133°. When the eruption started on September 5th the back azimuth increases from 63° to 72°. IE constantly points to about 128° intermittently changing to 134° with a small drop from 130° to 123°. This is pointing towards the south and might reflect noise from river Hverfisfljót. JO also mainly points to about 180°, but in August back azimuths are between 17° and 46°. Most of the energy comes from 46° between 16th and 24th of August (dyke intrusion at 50° to 60° from JO array) and 31st August to 5th September which is roughly the direction of the eruption.

Probable sub-glacial eruption & Sub-glacial flood: Tracking of tremor sources on September 3rd 2014 and June 2015. We managed to track a moving tremor sources and derive its migration speed, twice, beneath the glacier. On September 3rd 2014 we tracking magma and in May 2015 we tracked a flood from Grimsvotn caldera lake. We analysed the tremor burst on September 3rd (figure 6.3.6) not only with the seismic array UR but also applied an amplitude-based location method and numerical full wavefield simulations in order to constrain a horizontal and vertical source. Slownesses were in the range of 0.57 to 0.74 s/km during this tremor pulse which indicate a wavefield dominated by surface waves and a rather shallow source. The magmatic tremor source moved gradually southwards on September 3rd and could be located around the middle cauldron on Dyngjufjall glacier tongue probably leading to a subglacial eruption on that day. From the length of the tremor pulse, horizontal and

vertical source movement, we derived a velocity of 0.23 km/h or 0.06 m/s for this magmatic intrusion (figure 6.3.6).

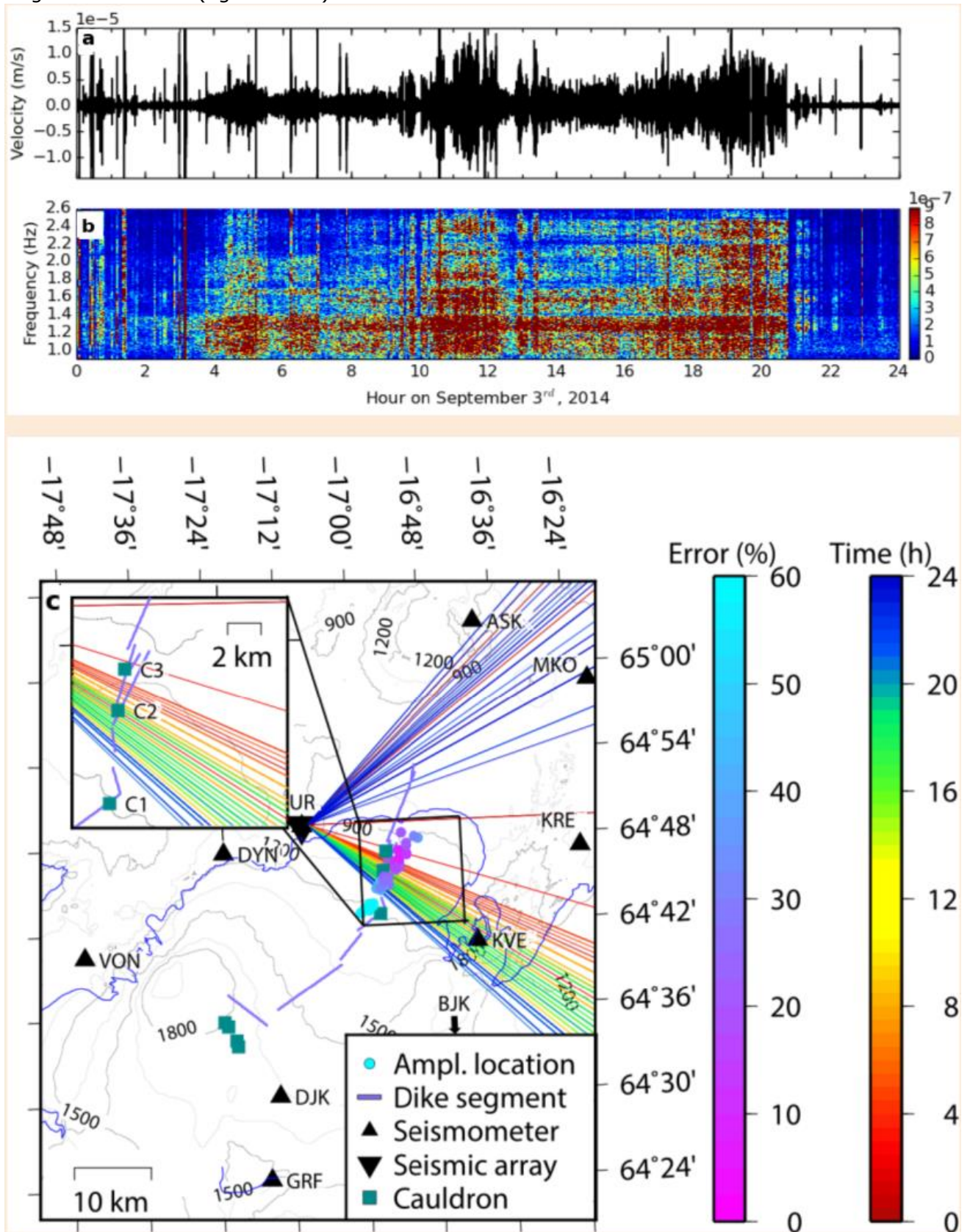


Fig. 6.3.6: (a) Seismogram at UR filtered between 0.9-2.6 Hz on September 3rd, 2014. (b) Spectrogram. (c) Lines represent the back azimuth at UR coloured according to time.

Dots represent the results from an amplitude-based location method using 10 stations from the Icelandic Met Office. Colours indicate the error at the best fitting location. The inset is a zoom to the region around the three cauldrons.

The tremor source during the flood from Grimvotn (figure 6.3.7) moved at about 1 km/h or 0.27 m/s and could be tracked with JO and IE array. We can therefore note that in this case the flood moved more than 3 times faster than the magma. But flood speeds strongly depend on the steepness of the flood path and can be lower as e.g. observed during subglacial floods from Katla volcano (Kristin Vogfjord, *Pers Com*)

When a tremor pulse occurs, magmatic and water sources have to be discriminated. Based on our analysis of known sources we can now say that flood tremor is usually stronger at higher frequencies, whereas magmatic tremor seems to dominate around 1 Hz. In the two cases shown in figure 6.3.6 and 6.3.7 the magmatic tremor was strongest around 1.3 Hz while the flood tremor was strongest from 2 to 4 Hz. The seismic data were filtered in two different frequency bands accordingly in figure 6.3.6 and 6.3.7. As noted, in this case we also saw the flood tremor migrating faster than the magma tremor (by a factor > 3), as expected in our original conceptual model for these processes (see introduction)

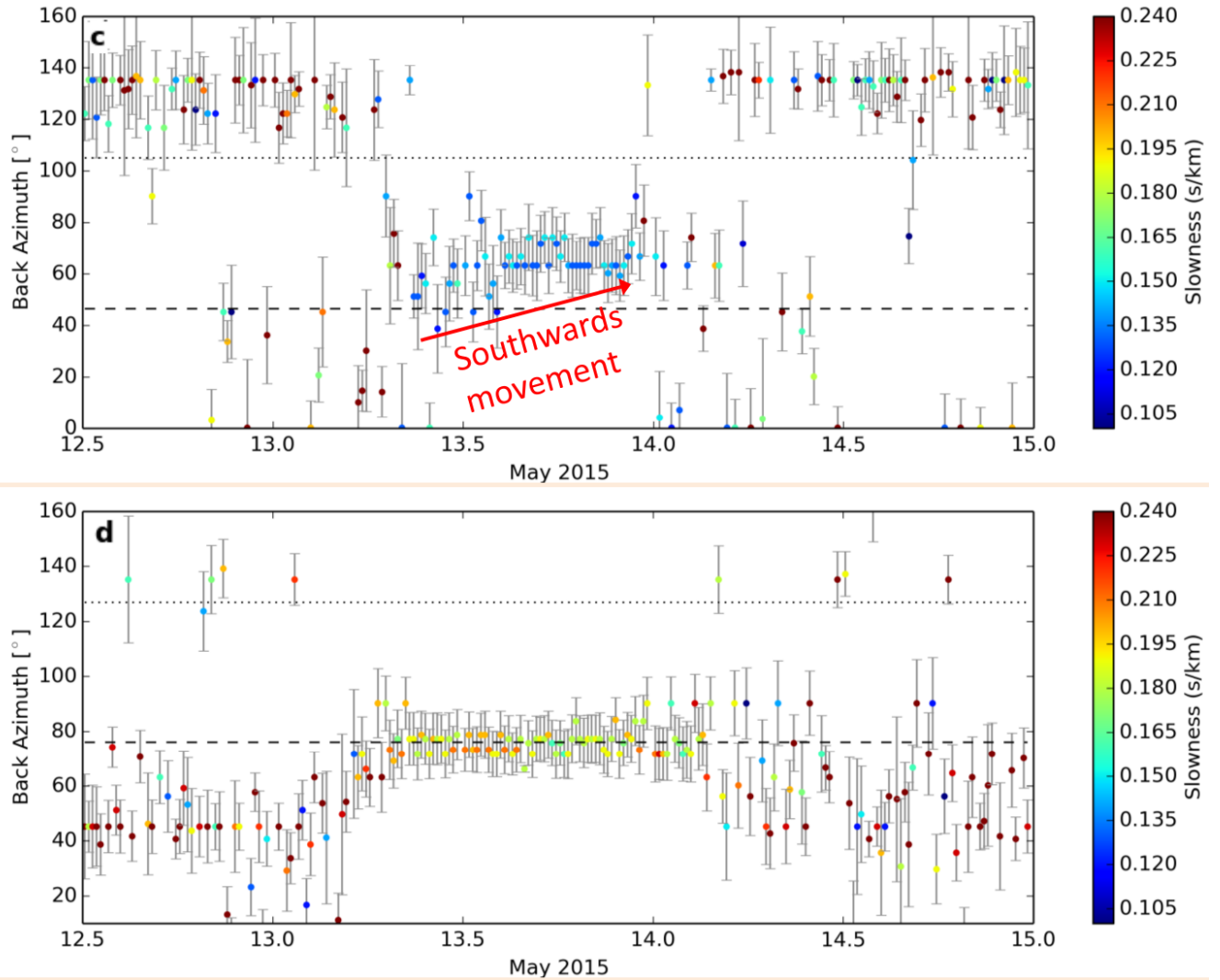


Figure 6.3.7: (c) Back azimuth at IE array coloured according to slowness when filtered to 2.4-4.2 Hz. Horizontal lines mark the back azimuth expected for signals from the Grimsvötn caldera (dashed) and at the outlet of Skeidararjökull (dotted). (d) Same as c but for JO array.

It can clearly be seen in figure 6.3.7 (d) that array analysis of flood related seismic tremor allows us to identify which outlet is active in the flooding episode over May 13-14th.

Note on a major tremor event from the eastern cauldron.

In October 2015 the eastern Skafta cauldron drained in one of the biggest jokulhlaups in the recent history as it had not drained for 5 years. The start of the flood was initially detected by a GPS instrument inside the cauldron. The seismic arrays in Jokulheimar and

Innri Eyrar detected tremor related to (i) lifting or breaking of ice, (ii) the outburst of the water from beneath the glacier, rupturing it and (iii) hydrothermal boiling in the cauldron once the water drained. Work to analyse this tremor is ongoing but is not yet complete. The analysis of this event will also include information from GPS instruments and water level measurements and will be part of the multi-disciplinary work in D6.6 (which is marginally delayed in order to allow this integration to take place – given that the flood only occurred in October).

Conclusions

Three seismic arrays capable of locating and tracking tremor were installed and tested. The tests took the form of a comparison of the locations and wavefield characteristic (e.g. slownesses) of a variety of earthquakes also located using the regional SIL seismic network. The arrays were also used to investigate tremor associated with magmatic processes, hydrothermal boiling and flood movement. Results can be summarised as follows:

- Array locations compare favourably with SIL epicentral locations for local earthquakes – hence we expect them to also perform well for seismic tremor locations.
- The range of earthquake depths, in association with 3D full wavefield numerical simulations, allowed us to calibrate the slowness measurements on the arrays in terms of source depths. This in turn allows us to estimate tremor depths using the arrays.
- Based on tremor analysis using the seismic arrays, it is almost certain that the dyke feeding the Holuhraun eruption reached the surface beneath the glacier causing a minor sub-glacial eruption on September 3rd, 2014
- Based on array tremor analysis using the arrays we can discriminate between magmatic processes and flooding processes both using spectral frequency (c. 1Hz for magmatic and c. 2-4Hz for floods) and tremor migration speeds (c. 0.23km/h for magmatic intrusion and c. 1km/h for flood, in the cases observed in this work)
- We were fortunate to record a major sub-glacial flood in October 2015, the data from which is still being analysed (in conjunction with GPS and water level data). It will be presented as part of D6.6, on multi-disciplinary work.
- In conclusion, all the goals associated with this deliverable have been fully realised, and a much clearer understanding of the nature of tremor in glacier covered volcanic environments is now available to front line interpreters.

Acknowledgements

We would like to thank those who assisted us with this work, especially Martin Möllhoff (UCD), Bergur Bergsson (IMO), Aoife Braiden (UCD) and Heiko Buxel (BGS) for their outstanding contributions in the field. Aoife Braiden for logistics and Martin Möllhoff for seismic data management.

References

- J. Almendros, R. Abella, M. M Mora, and P. Lesage. Array analysis of the seismic wavefield of long-period events and volcanic tremor at Arenal volcano, Costa Rica. *Journal of Geophysical Research: Solid Earth*, 119:1-24, 2014. doi: 10.1002/2013JB010628.
- J. Capon. High-Resolution Frequency-Wavenumber Spectrum Analysis. *Proceedings of the IEEE*, 57(8):1408-1418, 1969.
- Fiona A Darbyshire, I. Th Bjarnason, R. S White, and Ó. G Flóvenz. Crustal structure above the Iceland mantle plume imaged by the ICEMELT refraction profile. *Geophysical Journal International*, 135(3):1131-1149, 1998. doi: 10.1046/j.1365-246X.1998.00701.x.
- E Del Pezzo, M La Rocca, and J Ibanez. Observations of High-Frequency Scattered Waves Using Dense Arrays at Teide Volcano. *Bulletin of Seismological Society of America*, 87(6):1637-1647, 1997.
- Frankel, S. Hough, P. Friberg, and R. Busby. Observations of Loma Prieta aftershocks from a dense array in Sunnyvale, California. *Bulletin of the Seismological Society of America*, 00(5):1900-1922, 1991.
- P. Goldstein and R. J Archuleta. Array Analysis of Seismic Signals. *Geophysical Research Letters*, 14(1):13-16, 1987.
- S. Rost and C. Thomas. Array seismology: Methods and applications. *Reviews of Geophysics*, 40(3), 2002. ISSN 8755-1209. doi: 10.1029/2000RG000100.
- G Saccorotti and E Del Pezzo. A probabilistic approach to the inversion of data from a seismic array and its application to volcanic signals. *Geophysical Journal International*, 143:249-261, 2000.
- R. O Schmidt. Multiple Emitter Location and Signal Parameter Estimation. *IEEE Transactions on Antennas and Propagation*, AP-34(3):276-280, 1986.